Russian Chemical Bulletin, International Edition, Vol. 60, No. 12, pp. 2457—2469, December, 2011 2457

"Jumping" crystals: structures and properties of Cu^{II} complexes with *N*-methylimidazolyl- and *N*-methyltriazolyl-substituted nitronyl nitroxides

V. I. Ovcharenko,** *E. V. Tretyakov, S. V. Fokin, E. Yu. Fursova, O. V. Kuznetsova, S. E. Tolstikov, G. V. Romanenko, A. S. Bogomyakov, and R. Z. Sagdeev

International Tomography Center, Siberian Branch of the Russian Academy of Sciences,
3a ul. Institutskaya, 630090 Novosibirsk, Russian Federation.
Fax: +7 (383) 333 1399. E-mail: Victor.Ovcharenko@tomo.nsc.ru

To find the factors favorable for the appearance of chemomechanical activity of heterospin crystals, a series of new heterospin complexes were synthesized and characterized. It includes $[Cu(tfac)_2L^{Im}_2]\cdot 2CH_2Cl_2$, $[Cu(tfac)_2L^{Im}_2]\cdot 2EtOH$, $[[Cu(pfu)_2]_2L^{Im}_3]\cdot 1/2CH_2Cl_2$, $[Cu(pfh)_2L^{Im}_2]\cdot 1/2CH_2Cl_2$, $[Cu(piv)_2L^{Im}_2]\cdot 2MeOH$, $[Co(piv)_2L^{Im}_2]$, $[Cu(hfac)_2L^{CD_3}_2]$, $[Cu(hfac)_2L^{Tr}]_2\cdot CH_2Cl_2$, and $[Cu(hfac)_2L^{Tr}_2]$ (L^{Im}, L^{CD_3}, and L^{Tr} are *N*-methylimidazolyl-, *N*-trideuteriomethylimidazolyl-, and *N*-methyltriazolyl-substituted nitronyl nitroxides, respectively; tfac, hfac, pfu, pfh, and piv are the charged coordinated diamagnetic ligands 1,1,5,5-tetrafluoropentane-2,4-dionate, 1,1,1,5,5,5-hexafluoropentane-2,4-dionate, 1,1,1,2,2,3,3,4,4,8,8,9,9,10,10,11,11,11-octadecafluoroundecane-5,7-dionate, 1,1,1,5,5,6,6,6-octafluorohexane-2,4-dionate, and 2,2-dimethylpropionate, respectively). The crystal and molecular structures of all compounds were determined. The results of the X-ray diffraction study of the complex $[Ni(hfac)_2L^{Im}_2]$ synthesized earlier are reported. In the solid state of the complexes $[Cu(pfh)_2L^{Im}_2]$ and $[Co(piv)_2L^{Im}_2]$, the paramagnetic ligands are *cis*-coordinated to the central atom in a monodentate fashion *via* the donor N atom of the imidazole ring. In the dinuclear complexes $[[Cu(pfu)_2]_2L^{Im}_3]$ and $[Cu(hfac)_2L^{Tr}]_2$, the paramagnetic ligands are also in *cis* positions but act as bridges through coordination of the donor N atoms of the azole ring and the O atom of the nitronyl nitroxide moiety to different Cu^{2+} ions. In the solid complexes $[Cu(hfac)_2L^{CD_3}_2]$, $[Cu(hfac)_2L^{Tr}_2]$, $[Cu(tfac)_2L^{Im}_2]\cdot 2CH_2Cl_2$, $[Cu(tfac)_2L^{Im}_2]\cdot 2EtOH$, and $[Cu(piv)_2L^{Im}_2]\cdot 2MeOH$, the nitronyl nitroxide radicals in the mononuclear heterospin molecules are in *trans* positions. The packing motif in the crystal structures of the complexes $[Cu(hfac)_2L^{CD_3}_2]$, $[Cu(tfac)_2L^{Im}_2]\cdot 2CH_2Cl_2$, and $[Cu(tfac)_2L^{Im}_2]\cdot 2EtOH$ is the same as that in the previously studied complexes $[M(hfac)_2L^{Im}_2]$ exhibiting chemomechanical activity. Among the complexes under consideration, only crystals of $[Cu(hfac)_2L^{CD_3}_2]$ can exhibit chemomechanical activity, that is to make jumps upon heating or irradiation. The results of the present study suggest that the packing of the solid-state structure plays a key role in the generation of mechanical activity of the crystals.

Key words: copper(II) complexes, cobalt(II) complexes, nickel(II) complexes, coordination compounds, X-ray diffraction analysis, structure—property relationships, nitroxide radicals, hexafluoroacetylacetonates, pivalates.

Due to relatively high kinetic stability, 2-R-4,4,5,5-tetramethyl-2-imidazoline-3-oxide-1-oxyls (L^R) are readily available spin-labeled materials,[1—5] which are extensively used in the molecular design of magnets.[6—18] In the present study, we focused our attention on the characteristic features of this type of free radicals. Thus, even upon storage in the dark and at low temperature, all L^R gradually lose oxygen and are converted into the corresponding imino nitroxides at a particular rate. The same processes are observed for transition metal coordination compounds with L^R. Our experience in the work with these compounds shows that the solid-state heterospin complexes $[M(hfac)_2(L^R)_n]$ (M = Cu, Ni, Co, Mn; hfac is hexafluoroacetylacetonate) undergo gradual deoxygenation during storage for several years. At the macroscopic level, this is manifested in that the crystals of the complexes, primarily their surface, gradually lose quality. As a result, after long-term storage of the crystals of $[M(hfac)_2(L^R)_n]$ accompanied by their gradual deoxygenation, the crystals become non-transparent, change the color, and undergo cracking. The decomposition of $[M(hfac)_2(L^R)_n]$ occurs more rapidly in the light and at high temperatures.

The need to monitor the state of the crystals of $[M(hfac)_2(L^R)_n]$ prompted us to pay attention to unusual

---

Published in Russian in *Izvestiya Akademii Nauk. Seriya Khimicheskaya,* No. 12, pp. 2411—2422, December, 2011.

effects, which were observed for the first time for the heterospin complex [Cu(hfac)$_2$L^{Im}$_2$] (Im is *N*-methyl-1*H*-imidazol-5-yl). The elimination of O_2 from this compound is accompanied by the specific mechanical behavior of the crystals, the so-called jumps, due to sharp cracking of the crystals followed by rapid scattering of fragments. It can be supposed that oxygen is initially accumulated in cavities of the crystals, as in containers, and then it is sharply released, resulting in the crystal degradation. Individual crystals that are formed as a result of chemical fragmentation are scattered, which looks like jumps when watching with a microscope. Under ambient conditions, "jumps" and various displacements of crystals last for several weeks, mechanical movements leading to cracking and disintegration of the crystals. The observed mechanical effects are accompanied by a chemical reaction, during which the heterospin complex with nitronyl nitroxide is gradually transformed into the complex with the corresponding imino nitroxide radical. The longer the duration of mechanical movements of the ever-disintegrating crystals, the larger the percentage of the complex with the imino nitroxide radical in the solid state.[19]

To find the factors favorable for the appearance of chemomechanical activity of heterospins crystals, a group of complexes, in which the central atom was varied (M = Cu, Co, Ni, Mn), has been earlier synthesized and characterized.[19] Crystals of these complexes "jumped" under ambient conditions. The X-ray diffraction study of the complexes [Cu(hfac)$_2$L^{Im}$_2$], [Co(hfac)$_2$L^{Im}$_2$], and [Mn(hfac)$_2$L^{Im}$_2$] showed that these crystals are isostructural. It was also shown[19] that the change of the nature of the transition metal in the complexes [M(hfac)$_2$L^{Im}$_2$] has no effect on the possibility of the appearance of chemomechanical movement.

In continuation of our research on "jumping" crystals, we synthesized and characterized a series of Cu^{II} complexes with *N*-methylimidazolyl- and *N*-methyltriazolyl-substituted nitronyl nitroxides, which differ from the complexes [M(hfac)$_2$L^{Im}$_2$] in the structure of either the diamagnetic or paramagnetic ligand, as well as the Co^{II} pivalate complex with L^{Im}.

Results and Discussion

Synthesis of free radicals. In the present study, we used L^{Im}, its deuterated analog L^{CD_3}, and 2-(*N*-methyl-1,2,3-triazol-5-yl)-4,4,5,5-tetramethyl-2-imidazoline-3-oxide-1-oxyl (L^{Tr}) as paramagnetic ligands. The choice of the L^{CD_3} and L^{Tr} ligands was determined by the fact that the L^{Im} and L^{CD_3} ligands have virtually the same reactivity, and the molecular structure of the L^{Tr} ligand is topologically similar to that of L^{Im}. Taking into account the similarity of the spatial characteristics of the L^{CD_3} and L^{Tr} ligands to those of L^{Im}, the packing of the solid-state complexes [Cu(hfac)$_2$] with L^{CD_3} and L^{Tr} would be expected to be similar to that of the previously studied complexes [M(hfac)$_2$L^{Im}$_2$] exhibiting chemomechanical activity.

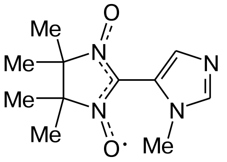

L^{Im}

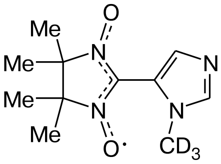

L^{CD_3}

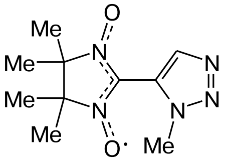

L^{Tr}

The reaction of $(CD_3)_2SO_4$ with imidazole-4(5)-carbaldehyde (**1**) in acetone afforded *N*-trideuteriomethylimidazole-5-carbaldehyde (**2**) (by analogy with *N*-methyl-1*H*-imidazole-5-carbaldehyde described earlier[20]) (Scheme 1). Then the condensation of aldehyde **2** with 2,3-dihydroxyamino-2,3-dimethylbutane (**3**) was performed, and the resulting product was oxidized in the MnO_2—MeOH system to prepare the target L^{CD_3}.

Scheme 1

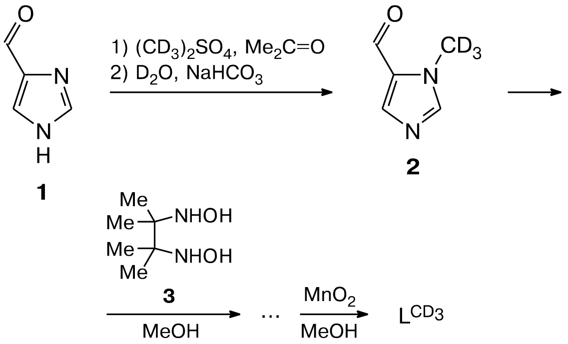

Nitronyl nitroxide L^{Tr} was synthesized with the use of dihydroxyamine **3** and aldehyde **4** as the starting reagents, whose condensation product (**5**) was oxidized with $NaIO_4$ in the two-phase CH_2Cl_2—H_2O system (Scheme 2).

Scheme 2

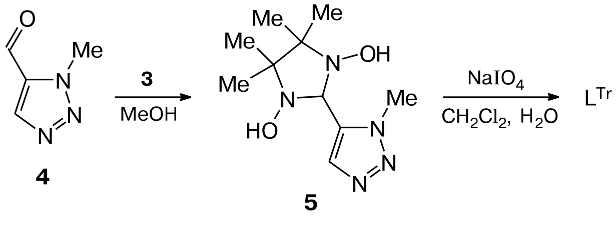

The presence of the $\mathrm{CD_3}$ group in $\mathrm{L^{CD_3}}$ is confirmed by the IR spectrum of the free radical, which shows bands at 2096 and 2152 $\mathrm{cm^{-1}}$ assigned to vibrations ν(C—D), as well as by the shift of the molecular ion peak and peaks of fragment ions bearing the $\mathrm{CD_3}$ group to larger values by 3 amu in the mass spectrum of $\mathrm{L^{CD_3}}$ compared to the mass spectrum of $\mathrm{L^{Im}}$. The free-radical character of $\mathrm{L^{CD_3}}$ and $\mathrm{L^{Tr}}$ is evidenced by their effective magnetic moments (μ_{eff}), which are virtually unchanged (1.73 μ_{B}) in the temperature range of 200—300 K.

Synthesis of complexes. To elucidate the influence of the ligand environment on the possibility of the appearance of chemomechanical activity in crystals of heterospin complexes, it was of interest to vary the metal-containing moiety. For this reason, we synthesized new compounds with the use of fluorinated analogs of $\mathrm{[Cu(hfac)_2]}$, *viz.*, bis(1,1,5,5-tetrafluoropentane-2,4-dionato)copper(II) ($\mathrm{[Cu(tfac)_2]}$), bis(1,1,1,5,5,6,6,6-octafluorohexane-2,4-dionato)copper(II) ($\mathrm{[Cu(pfh)_2]}$), and bis(1,1,1,2,2,3,3,4,4,8,8,9,9,10,10,11,11,11-octadecafluoroundecane-5,7-dionato)copper(II) ($\mathrm{[Cu(pfu)_2]}$), as well as the pivalate complexes $\mathrm{[Cu_2(piv)_4(THF)_2]}$ and $\mathrm{[Co_2(piv)_4(H_2O)(Hpiv)_4]}$ (piv is 2,2-dimethylpropionate), which are readily soluble in nonpolar organic solvents and contain easily replaceable monodentate ligands (THF, Hpiv).

The bischelates $\mathrm{[Cu(tfac)_2]}$, $\mathrm{[Cu(pfh)_2]}$, and $\mathrm{[Cu(pfu)_2]}$ were prepared by the dehydration of the aqua complexes $\mathrm{[CuL_2(H_2O)]}$ (L is tfac, pfh, or pfu, respectively), which were, in turn, synthesized by the reaction of $\mathrm{[Cu(OAc)_2(H_2O)]_2}$ with the corresponding β-diketone in water in the presence of NaOH.

The heterospin complexes $\mathrm{[Cu(hfac)_2L^{CD_3}{}_2]}$, $\mathrm{[Cu(tfac)_2L^{Im}{}_2]\cdot 2CH_2Cl_2}$, and $\mathrm{[Cu(pfh)_2L^{Im}{}_2]\cdot 1/2CH_2Cl_2}$ were synthesized under the same conditions as the complex $\mathrm{[Cu(hfac)_2L^{Im}{}_2]}$,[19] *i.e.*, by the reaction of $\mathrm{[CuL_2]}$ with the corresponding nitronyl nitroxide in a mixture of EtOH and $\mathrm{CH_2Cl_2}$ taken in the ratio $\mathrm{[CuL_2] : L^R = 1 : 2}$. We failed to synthesize the complex $\mathrm{[Cu(pfu)_2]}$ with two radicals $\mathrm{L^{Im}}$ under similar conditions. In spite of the use of the starting reagents in the ratio of 1 : 2, the recrystallization of the reaction product from EtOH always resulted in the formation of the complex $\mathrm{[[Cu(pfu)_2]_2L^{Im}{}_3]\cdot 1/2CH_2Cl_2}$ as the solid phase. The ethanol solvate $\mathrm{[Cu(tfac)_2L^{Im}{}_2]\cdot 2EtOH}$ was formed in the reaction of $\mathrm{[Cu(tfac)_2]}$ with $\mathrm{L^{Im}}$ in EtOH.

It is impossible to use the similar approach for the synthesis of complexes with nitronyl nitroxide $\mathrm{L^{Tr}}$, because the crystallization from an EtOH—$\mathrm{CH_2Cl_2}$ mixture gave the free radical as the solid phase. The solvate $\mathrm{[Cu(hfac)_2L^{Tr}]_2\cdot CH_2Cl_2}$ and the complex $\mathrm{[Cu(hfac)_2L^{Tr}{}_2]}$ were crystallized from a heptane—$\mathrm{CH_2Cl_2}$ mixture.

The mononuclear complexes $\mathrm{[Cu(piv)_2L^{Im}{}_2]\cdot 2MeOH}$ and $\mathrm{[Co(piv)_2L^{Im}{}_2]}$ with the ratio $\mathrm{M : L^{Im} = 1 : 2}$ containing coordinated pivalates instead of hexafluoroacetylacetonates were synthesized by the reaction of $\mathrm{L^{Im}}$ with the dinuclear complexes $\mathrm{[Cu_2(piv)_4(THF)_2]}$ and $\mathrm{[Co_2(piv)_4(H_2O)(Hpiv)_4]}$, respectively.

Structures of compounds. All the coordination compounds under consideration, as well as the $\mathrm{L^{CD_3}}$ and $\mathrm{L^{Tr}}$ ligands, were grown as single crystals, which were studied by X-ray diffraction. The crystallographic characteristics of the compounds and the X-ray data collection statistics are summarized in Tables 1—3. Selected bond lengths and bond angles are listed in Tables 4 and 5.

The structures of the paramagnetic $\mathrm{L^{CD_3}}$ and $\mathrm{L^{Tr}}$ ligands and the complexes $\mathrm{[Cu(pfh)_2L^{Im}{}_2]}$,

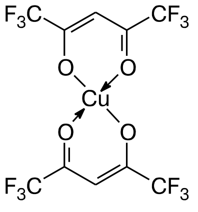

$\mathrm{[Cu(hfac)_2]}$

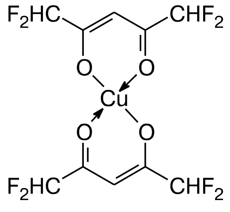

$\mathrm{[Cu(tfac)_2]}$

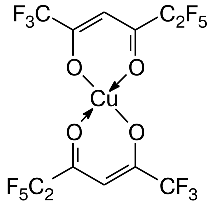

$\mathrm{[Cu(pfh)_2]}$

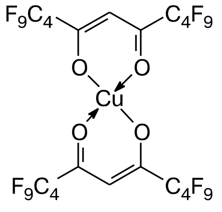

$\mathrm{[Cu(pfu)_2]}$

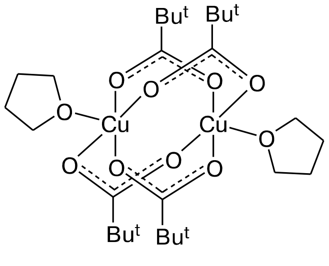

$\mathrm{[Cu_2(piv)_4(THF)_2]}$

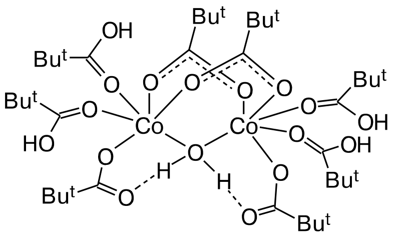

$\mathrm{[Co_2(piv)_4(H_2O)(Hpiv)_4]}$

Table 1. Crystallographic characteristics and the X-ray data collection statistics for the L^{CD_3} and L^{Tr} ligands, their complexes, and the complex $[Ni(hfac)_2L^{Im}{}_2]$

Parameter	$L^{CD_3}\cdot 1/2H_2O$	L^{Tr}	$[Cu(hfac)_2L^{CD_3}{}_2]$	$[Ni(hfac)_2L^{Im}{}_2]$	$[Cu(hfac)_2L^{Tr}]_2\cdot CH_2Cl_2$	$[Cu(hfac)_2L^{Tr}{}_2]$
M	246.29	238.28	958.26	972.40	1518.80	954.21
T/K	240	240	240	240	240	240
Space group	$P\bar{1}$	$P\bar{1}$	$P\bar{1}$	$P\bar{1}$	$C2/c$	$P\bar{1}$
Z	1	2	1	1	4	2
a/Å	7.2146(6)	7.091(2)	7.0824(6)	7.1132(17)	29.2048(17)	10.0869(5)
b/Å	13.5437(9)	9.877(3)	11.4489(9)	11.243(3)	10.5518(6)	10.4091(5)
c/Å	13.8504(9)	9.877(3)	12.8085(9)	13.012(3)	20.7411(12)	11.4259(9)
α/deg	88.104(5)	93.395(1)	101.655(3)	102.183(7)	—	110.346(4)
β/deg	79.307(6)	110.226(4)	99.708(3)	99.701(7)	105.246(4)	113.327(4)
γ/deg	83.090(5)	110.226(4)	100.643(4)	99.531(7)	—	98.936(3)
V/Å^3	1320.12(16)	596.5(3)	976.52(13)	980.5(4)	6166.7(6)	971.22(10)
d_{calc}/g cm^{-3}	1.239	1.327	1.629	1.604	1.636	1.631
μ/mm^{-1}	0.090	0.097	0.676	0.611	0.910	0.682
θ_{min}—θ_{max}/deg	1.50—27.97	2.24—29.18	1.66—30.51	1.64—27.48	2.76—28.33	2.22—28.07
Number of measured /independent reflections	22780/6325	4425/2339	20669/5801	15294/4359	20774/7536	14077/4624
R_{int}	0.1147	0.1617	0.0945	0.1048	0.1420	0.0681
N	461	155	386	323	503	332
GOOF	0.780	0.858	0.941	1.073	0.706	0.952
R_1	0.0479	0.0645	0.0425	0.0657	0.0546	0.0424
wR_2 ($I > 2\sigma(I)$)	0.0904	0.1394	0.0956	0.1998	0.1025	0.0935

Table 2. Crystallographic characteristics and the X-ray data collection statistics for the complexes $[Cu(tfac)_2(H_2O)]$, $[Cu(pfh)_2]$, $[Cu(tfac)_2L^{Im}{}_2]\cdot 2CH_2Cl_2$, and $[Cu(tfac)_2L^{Im}{}_2]\cdot 2EtOH$

Parameter	$[Cu(tfac)_2(H_2O)]$	$[Cu(pfh)_2]$	$[Cu(tfac)_2L^{Im}{}_2]\cdot 2CH_2Cl_2$	$[Cu(tfac)_2L^{Im}{}_2]\cdot 2EtOH$
M	423.70	577.68	1050.11	972.40
T/K	240	240	295	240
Space group	$P2_1/n$	$P\bar{1}$	$P\bar{1}$	$P\bar{1}$
Z	4	1	1	1
a/Å	15.1896(17)	5.181(2)	7.1299(4)	7.1019(6)
b/Å	5.7814(7)	8.306(3)	12.2222(8)	12.1608(13)
c/Å	15.720(2)	10.928(4)	13.2073(8)	13.0714(11)
α/deg	—	104.65(2)	86.684(4)	86.591(7)
β/deg	91.731(7)	95.06(3)	74.826(4)	74.559(6)
γ/deg	—	98.91(3)	85.180(4)	83.443(6)
V/Å^3	1379.8(3)	445.5(3)	1106.10(12)	1080.55(17)
d_{calc}/g cm^{-3}	2.040	2.153	1.576	1.494
μ/mm^{-1}	1.703	1.408	0.826	0.603
θ_{min}—θ_{max}/deg	2.59—27.51	1.94—28.22	1.60—28.36	2.37—28.156
Number of measured /independent reflections	11420/3124	5491/2016	17303/5390	11268/5145
R_{int}	0.0891	0.1656	0.1173	0.1189
N	275	178	314	286
GOOF	0.765	0.893	0.940	0.766
R_1	0.0438	0.0694	0.0757	0.0560
wR_2 ($I > 2\sigma(I)$)	0.0677	0.1695	0.1896	0.1010

Table 3. Crystallographic characteristics and the X-ray data collection statistics for the complexes $[[Cu(pfu)_2]_2L^{Im}{}_3]\cdot 1/2CH_2Cl_2$, $[Cu(pfh)_2L^{Im}{}_2]\cdot 1/2CH_2Cl_2$, $[Cu(piv)_2L^{Im}{}_2]\cdot 2MeOH$, and $[Co(piv)_2L^{Im}{}_2]$

Parameter	$[[Cu(pfu)_2]_2L^{Im}{}_3]\cdot 1/2CH_2Cl_2$	$[Cu(pfh)_2L^{Im}{}_2]\cdot 1/2CH_2Cl_2$	$[Cu(piv)_2L^{Im}{}_2]\cdot 2MeOH$	$[Co(piv)_2L^{Im}{}_2]$
M	2909.88	1094.71	804.44	735.75
T/K	240	240	295	295
Space group	$P\bar{1}$	$P\bar{1}$	$P\bar{1}$	$C2/c$
Z	2	2	1	4
a/Å	13.7244(8)	9.8380(4)	7.201(5)	22.759(7)
b/Å	15.7137(8)	14.3853(7)	11.971(9)	6.928(2)
c/Å	27.5781(13)	17.7252(7)	12.605(9)	24.033(7)
α/deg	95.471(4)	95.234(3)	98.825(12)	—
β/deg	93.290(4)	92.555(3)	99.590(13)	98.608(4)
γ/deg	105.447(4)	106.803(3)	100.284(12)	—
V/Å^3	5685.3(5)	2384.77(18)	1035(1)	3747(2)
d_{calc}/g cm^{-3}	1.700	1.525	1.290	1.304
μ/mm^{-1}	0.576	0.631	0.588	0.515
θ_{min}—θ_{max}/deg	1.35—28.02	1.78—28.08	2.19—23.38	1.81—23.32
Number of measured /independent reflections	60319/27086	33417/11316	7810/2970	13665/2704
R_{int}	0.2046	0.1161	0.0415	0.0484
N	1608	731	268	222
GOOF	0.641	0.904	1.054	1.268
R_1	0.0866	0.0768	0.0464	0.0468
wR_2 ($I > 2\sigma(I)$)	0.2176	0.2068	0.1194	0.1235

Table 4. Selected bond lengths (d) and the CN_2—Im(Tr) bond angles (τ) in the L^{CD_3} and L^{Tr} molecules and the complexes $[Cu(hfac)_2L^{CD_3}{}_2]$, $[Ni(hfac)_2L^{Im}{}_2]$, $[Cu(hfac)_2L^{Tr}]_2\cdot CH_2Cl_2$, and $[Cu(hfac)_2L^{Tr}{}_2]$

Compound	d/Å				τ/deg
	M—O	M—O_{NO}	M—N	N—O	
$L^{CD_3}\cdot 1/2H_2O$	—	—	—	1.278(2)—1.283(2)	41.5(2)—38.4(2)
L^{Tr}	—	—	—	1.271(5), 1.282(4)	45.7(4)
$[Cu(hfac)_2L^{CD_3}{}_2]$	1.9874(12), 2.3159(13)	—	2.0079(13)	1.275(2), 1.274(2)	45.88(8)
$[Ni(hfac)_2L^{Im}{}_2]$	2.033(3), 2.059(4)	—	2.078(4)	1.273(5), 1.283(5)	44.8(6)
$[Cu(hfac)_2L^{Tr}]_2\cdot$ $\cdot CH_2Cl_2$	1.934(2)—1.947(2), 2.281(2)	2.458(2)	1.992(3)	1.281(3), 1.274(3)	54.3(2)
$[Cu(hfac)_2L^{Tr}{}_2]$	1.9941(14), 2.2963(15)	—	2.0191(15)	1.280(2), 1.268(2)	34.9(1)

Note. M = Cu, Ni.

Table 5. Selected bond lengths (d) and the CN_2—Im bond angles (τ) in the complexes $[Cu(tfac)_2(H_2O)]$, $[Cu(pfh)_2]$, $[Cu(tfac)_2L^{Im}{}_2]\cdot 2CH_2Cl_2$, $[Cu(tfac)_2L^{Im}{}_2]\cdot 2EtOH$, $[Cu(pfh)_2L^{Im}{}_2]\cdot 1/2CH_2Cl_2$, $[Cu(piv)_2L^{Im}{}_2]\cdot 2MeOH$, and $[Co(piv)_2L^{Im}{}_2]$

Complex	d/Å			τ/deg
	Cu—O	Cu—N	N—O	
$[Cu(tfac)_2(H_2O)]$	1.935(2)—1.950(2), 2.310(3)	—	—	—
$[Cu(pfh)_2]$	1.890(5), 1.921(4)	—	—	—
$[Cu(tfac)_2L^{Im}{}_2]\cdot 2CH_2Cl_2$	1.987(3), 2.284(3)	2.024(3)	1.257(4), 1.271(4)	53.9(3)
$[Cu(tfac)_2L^{Im}{}_2]\cdot 2EtOH$	1.978(3), 2.321(3)	2.028(3)	1.271(4), 1.288(4)	55.5(4)
$[Cu(pfh)_2L^{Im}{}_2]\cdot 1/2CH_2Cl_2$	1.979(4), 1.987(4), 2.299(4), 2.310(4)	1.975(4), 2.002(4)	1.292(5), 1.274(5), 1.269(5), 1.283(5)	42.8(2), 53.3(2)
$[Cu(piv)_2L^{Im}{}_2]\cdot 2MeOH$	1.940(3)	1.984(3)	1.272(3), 1.279(3)	38.4(3)
$[Co(piv)_2L^{Im}{}_2]$	2.121(2), 2.207(2)	2.088(2)	1.273(3), 1.269(3)	48.7(1)

$[[Cu(pfu)_2]_2L^{Im}{}_3]$, $[Cu(hfac)_2L^{Tr}]_2$, and $[Co(piv)_2L^{Im}{}_2]$ are shown in Fig. 1.* The geometry of the molecules $[Cu(pfh)_2L^{Im}{}_2]$, $[[Cu(pfu)_2]_2L^{Im}{}_3]$, $[Cu(hfac)_2L^{Tr}]_2$, and $[Co(piv)_2L^{Im}{}_2]$ substantially differs from that of the molecule $[Cu(hfac)_2L^{Im}{}_2]$ (Fig. 2, *a*) containing the monodentate L^{Im} ligands in *trans* positions. In the complexes

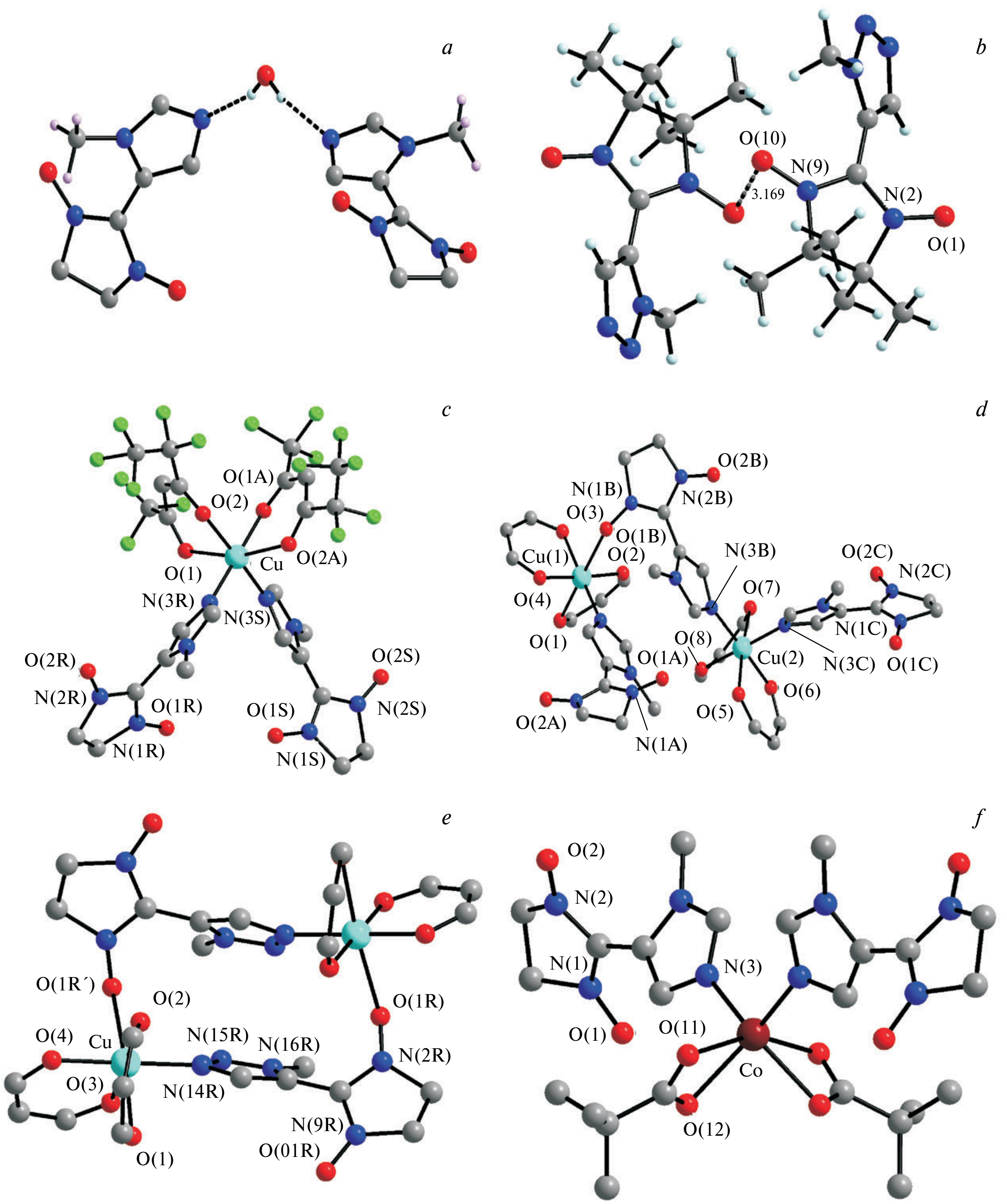

Fig. 1. Molecular structures of $L^{CD_3} \cdot 1/2H_2O$ (*a*), L^{Tr} (*b*), $[Cu(pfh)_2L^{Im}{}_2]$ (*c*), $[[Cu(pfu)_2]_2L^{Im}{}_3]$ (*d*), $[Cu(hfac)_2L^{Tr}]_2$ (*e*), and $[Co(piv)_2L^{Im}{}_2]$ (*f*).

---

* Figures 1—4 are available in full color in the on-line version of the journal (http://www.springerlink.com/fulltext.pdf).

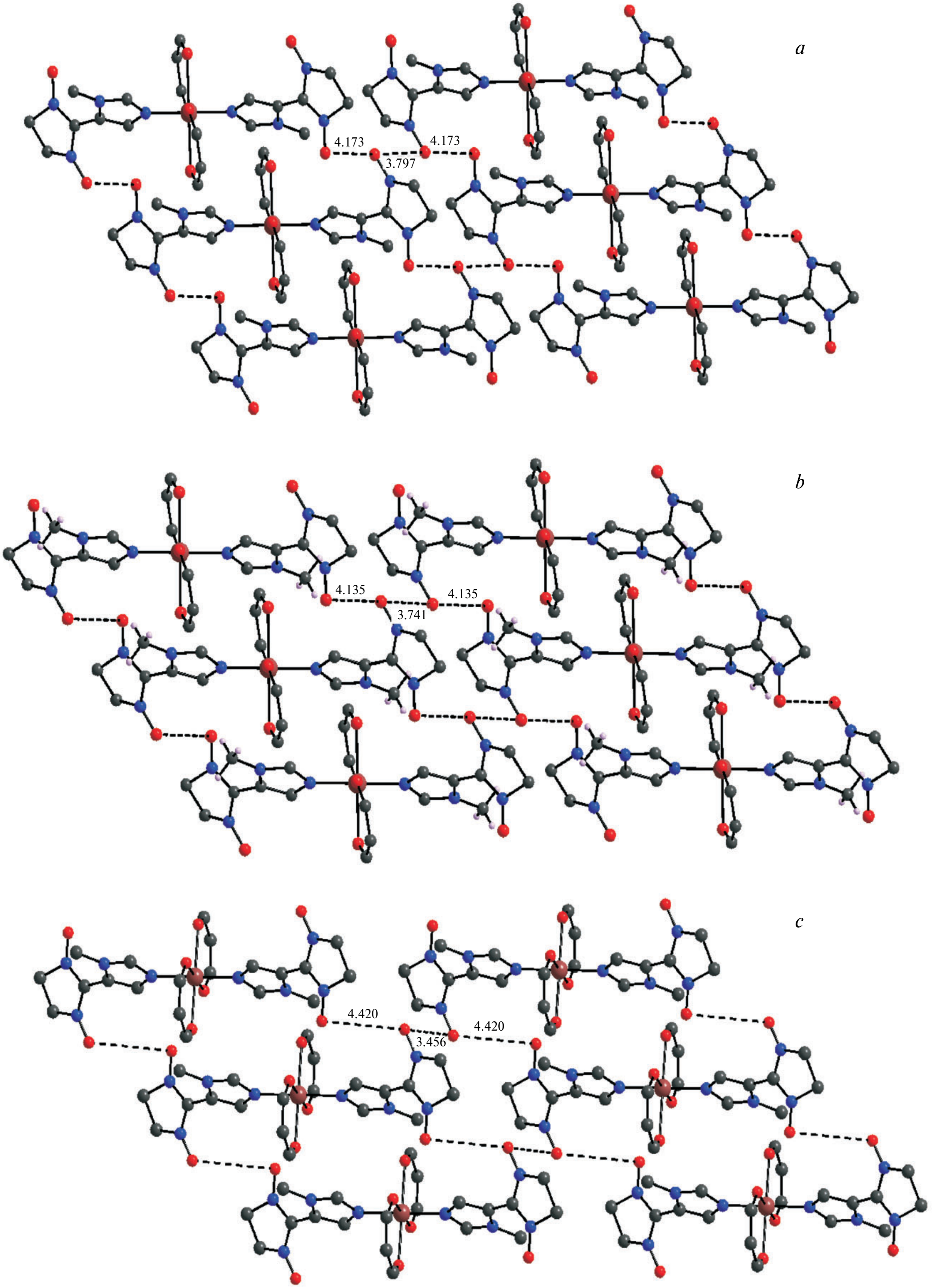

Fig. 2. Molecular packing in the crystal structures of the complexes [Cu(hfac)$_2$L$^{\mathrm{Im}}{}_2$] (*a*), [Cu(hfac)$_2$L$^{\mathrm{CD_3}}{}_2$] (*b*), and [Cu(tfac)$_2$L$^{\mathrm{Im}}{}_2$] $\cdot$ 2CH$_2$Cl$_2$ (*c*).

[Cu(pfh)$_2$L$^{\mathrm{Im}}{}_2$] and [Co(piv)$_2$L$^{\mathrm{Im}}{}_2$] (see Fig. 1, *c* and *f*), the monodentate L$^{\mathrm{Im}}$ ligands are in *cis* positions, whereas the *cis*-coordinated paramagnetic ligands in the dinuclear complexes [[Cu(pfu)$_2$]$_2$L$^{\mathrm{Im}}{}_3$] and [Cu(hfac)$_2$L$^{\mathrm{Tr}}$]$_2$ (see Fig. 1, *d* and *e*) are involved in the bridging coordination (one ligand in [[Cu(pfu)$_2$]$_2$L$^{\mathrm{Im}}{}_3$] and two ligands in

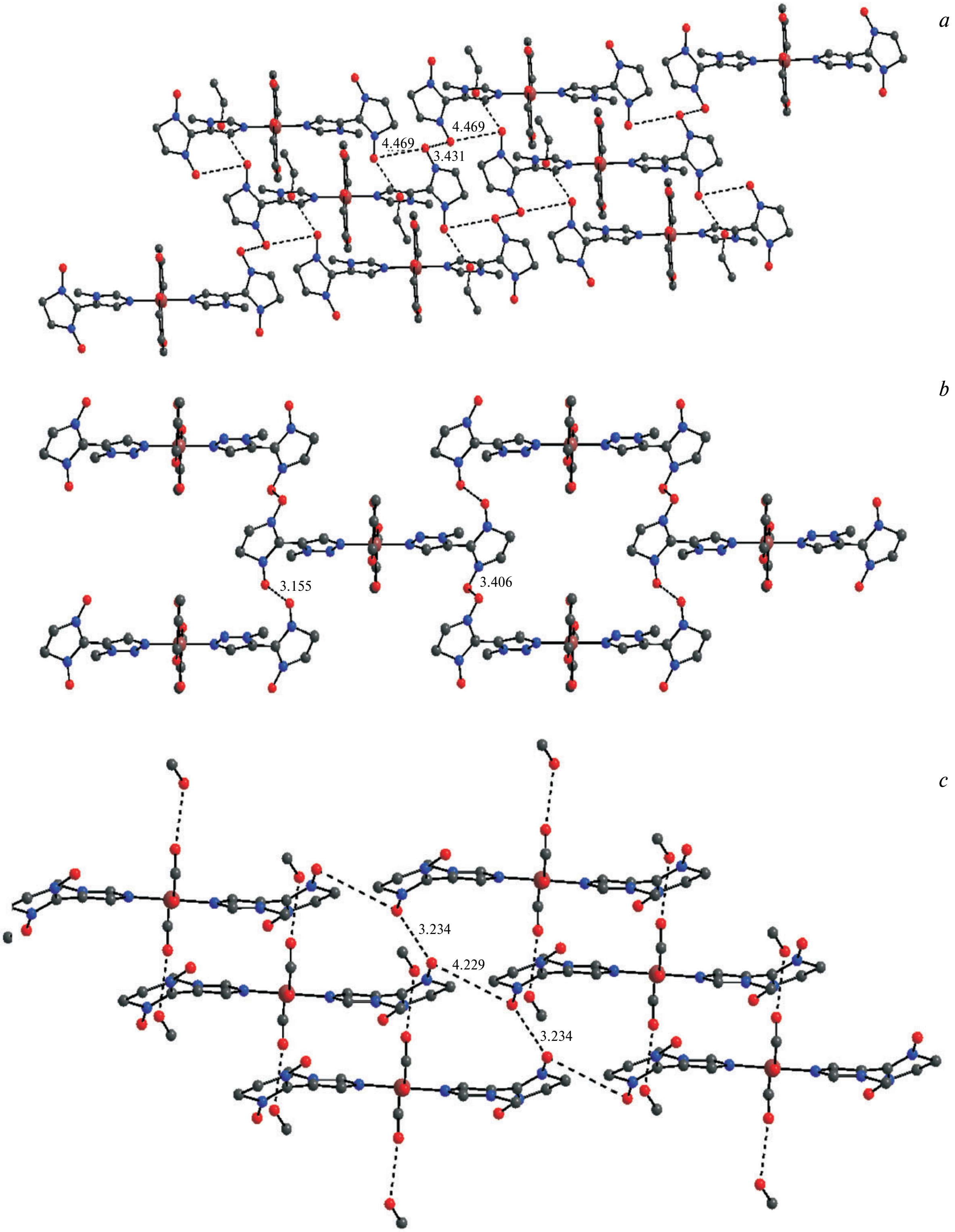

Fig. 3. Molecular packing in the crystal structures of the complexes [Cu(tfac)$_2$L$^{\mathrm{Im}}{}_2$]$\cdot$2EtOH (*a*), [Cu(hfac)$_2$L$^{\mathrm{Tr}}{}_2$] (*b*), and [Cu(piv)$_2$L$^{\mathrm{Im}}{}_2$]$\cdot$2MeOH (*c*).

$[Cu(hfac)_2L^{Tr}{}_2]$). Since the packing of these compounds cannot be, in principle, the same as that of $[M(hfac)_2L^{Im}{}_2]$, these compounds would not be expected to exhibit chemomechanical activity. This was confirmed experimentally. Thus, the observation of the behavior of the single crystals of these complexes in the light or during heating did not reveal any mechanical activity. Hence, we will not discuss these complexes in more detail.

For the aims of the present study, the structures of the complexes $[Cu(hfac)_2L^{CD_3}{}_2]$, $[Cu(hfac)_2L^{Tr}{}_2]$, $[Cu(tfac)_2L^{Im}{}_2] \cdot 2CH_2Cl_2$, $[Cu(tfac)_2L^{Im}{}_2] \cdot 2EtOH$, and $[Cu(piv)_2L^{Im}{}_2] \cdot 2MeOH$ are of much more interest, because they have the same composition as the complex $[Cu(hfac)_2L^{Im}{}_2]$ and also contain *trans*-coordinated paramagnetic ligands in the heterospin molecule (see Figs 2 and 3). Moreover, the donor N atoms of the azole ring in the complexes, in which Cu^{II} is in a distorted octahedral environment, *viz*., $[Cu(hfac)_2L^{CD_3}{}_2]$, $[Cu(hfac)_2L^{Tr}{}_2]$, $[Cu(tfac)_2L^{Im}{}_2] \cdot 2CH_2Cl_2$, and $[Cu(tfac)_2L^{Im}{}_2] \cdot 2EtOH$, are in equatorial positions, like in the complex $[Cu(hfac)_2L^{Im}{}_2]$ (see Tables 4 and 5). Hence, this group of complexes would be expected to have the similar molecular packing in the solid phase as in $[Cu(hfac)_2L^{Im}{}_2]$.

Actually, the packing of $[Cu(hfac)_2L^{Im}{}_2]$ differs only slightly from that of $[Cu(hfac)_2L^{CD_3}{}_2]$ (see Fig. 2, *a* and *b*). Hence, it is not surprising that the crystals of $[Cu(hfac)_2L^{CD_3}{}_2]$, like the crystals of $[Cu(hfac)_2L^{Im}{}_2]$, have a nontrivial feature. At room temperature, the chaotic movement of the bulk of crystals of the complex $[Cu(hfac)_2L^{CD_3}{}_2]$ placed in a Petri dish was visually observed, and their "jumps" were seen when watching with a usual microscope. These jumps of the crystals were activated upon heating to ~28—32 °C, and they became more intense when a source of visible light (a table lamp or a light guide) was brought close to the crystals. "Jumps" almost completely stopped when the Petri dish with the crystals was placed in a refrigerator. When warmed again to room temperature, the crystals began to "jump" again. The cooling and warming of the crystals of $[Cu(hfac)_2L^{CD_3}{}_2]$ can be repeated many times, and the same phenomenon was observed for these crystals, like for the crystals of $[Cu(hfac)_2L^{Im}{}_2]$, *e.g*., they made "jumps" upon heating or under irradiation.

Therefore, in the case of the isotope substitution (the replacement of the CH_3 group by the CD_3 group in the paramagnetic ligand), the packing and chemomechanical activity of the crystals remain unchanged on going from $[Cu(hfac)_2L^{Im}{}_2]$ to $[Cu(hfac)_2L^{CD_3}{}_2]$. It should also be noted that the intra- and intermolecular distances and the bond angles in the complexes $[Cu(hfac)_2L^{Im}{}_2]$ and $[Cu(hfac)_2L^{CD_3}{}_2]$ are statistically different, when comparing the data obtained at the same temperature (Table 6). A comparison of the structural characteristics of the complexes evaluated at different temperatures shows that the geometric parameters of the complex $[Cu(hfac)_2L^{CD_3}{}_2]$ are similar to those of the complex $[Cu(hfac)_2L^{Im}{}_2]$ at higher temperature. Thus, the bond lengths and bond angles in $[Cu(hfac)_2L^{CD_3}{}_2]$ are more similar to those in $[Cu(hfac)_2L^{Im}{}_2]$ determined at 305 K than at 240 K (see Table 6).

Table 6. Selected bond lengths and the CN_2—Im bond angles in the complexes $[Cu(hfac)_2L^{Im}{}_2]$ and $[Cu(hfac)_2L^{CD_3}{}_2]$ at different temperatures

Parameter	$[Cu(hfac)_2L^{Im}{}_2]$		$[Cu(hfac)_2L^{CD_3}{}_2]$ 240 K
	305 K	240 K	
Bond/Å			
Cu—O	1.995(2), 2.292(3)	1.965(4), 2.274(4)	1.9874(12), 2.3159(13)
$Cu—N_{Im}$	1.998(3)	1.977(5)	2.0079(13)
N—O	1.278(4), 1.272(4)	1.261(6), 1.265(6)	1.275(2), 1.274(2)
Angle/deg			
CN_2—Im	45.8(2)	44.7(3)	45.88(8)

The molecular packing in the crystals of $[Cu(hfac)_2L^{Tr}{}_2]$ and $[Cu(piv)_2L^{Im}{}_2] \cdot 2MeOH$ (see Fig. 3, *b* and *c*) is substantially different from that in $[Cu(hfac)_2L^{Im}{}_2]$ or $[Cu(hfac)_2L^{CD_3}{}_2]$. For example, the molecular packing in $[Cu(hfac)_2L^{Im}{}_2]$ and $[Cu(hfac)_2L^{CD_3}{}_2]$ is such that the O atoms of the nitronyl nitroxide moiety are arranged in quadruples with the short central O...O distance, longer terminal distances, and ever-longer distances between the quadruples (see Fig. 2, *a* and *b*). In the solid complexes $[Cu(hfac)_2L^{Tr}{}_2]$ and $[Cu(piv)_2L^{Im}{}_2] \cdot 2MeOH$, there are no such quadruples. Hence, it is not surprising that the complexes $[Cu(hfac)_2L^{Tr}{}_2]$ and $[Cu(piv)_2L^{Im}{}_2] \cdot 2MeOH$ do not exhibit chemomechanical activity inherent in the complexes $[Cu(hfac)_2L^{Im}{}_2]$ and $[Cu(hfac)_2L^{CD_3}{}_2]$.

The packing of the solvates $[Cu(tfac)_2L^{Im}{}_2] \cdot 2CH_2Cl_2$ and $[Cu(tfac)_2L^{Im}{}_2] \cdot 2EtOH$ (see Fig. 2, *c* and 3, *a*) are of much more interest. In these crystals, the molecules are arranged in layers identical to those observed in $[Cu(hfac)_2L^{Im}{}_2]$ or $[Cu(hfac)_2L^{CD_3}{}_2]$. In the layers, there are identical groups formed by four O atoms of the nitronyl nitroxide moieties. The O atoms in these quadruples are linked by dashed lines, above which the interatomic distances are given (see Figs 2, *a*—*c* and 3, *a*). However, the layers of the heterospin molecules in the solid-state complexes $[Cu(tfac)_2L^{Im}{}_2] \cdot 2CH_2Cl_2$ and $[Cu(tfac)_2L^{Im}{}_2] \cdot 2EtOH$ are separated by solvent molecules (Fig. 4). The inclusion of solvent molecules has a substantial effect on the mechanical properties of the crystals of these compounds. For these compounds, the chemomechanical activity inherent in the crystals of $[Cu(hfac)_2L^{Im}{}_2]$ and $[Cu(hfac)_2L^{CD_3}{}_2]$ was not observed.

Therefore, based on the results of the present study, an important conclusion can be made that the above-de-

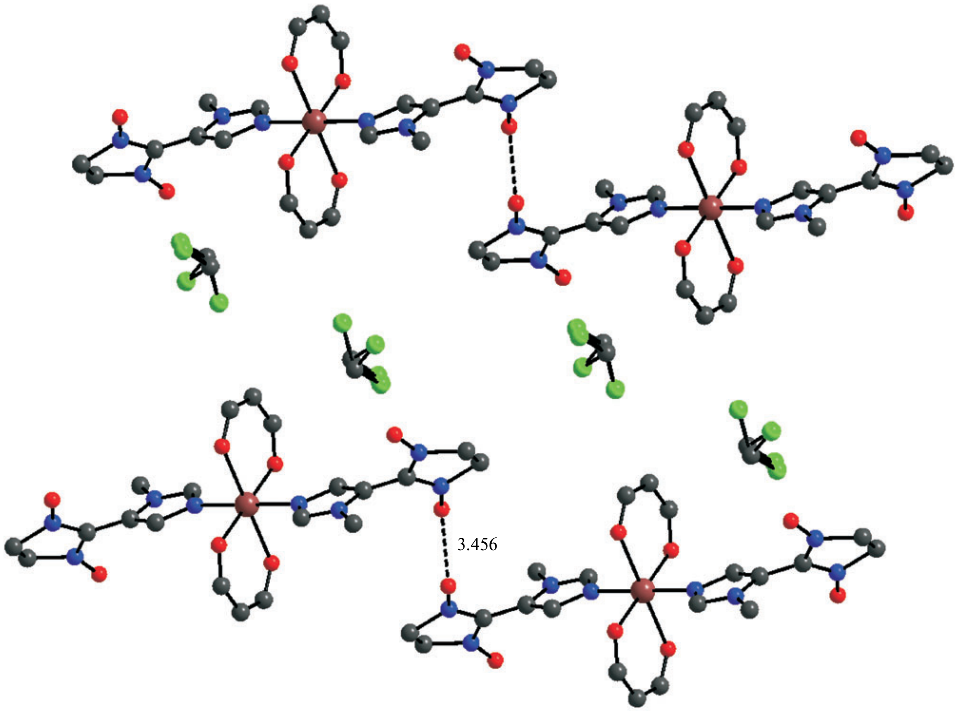

Fig. 4. Disordered CH_2Cl_2 molecules located between the layers in the crystal structure of $[Cu(tfac)_2L^{Im}{}_2] \cdot 2CH_2Cl_2$.

scribed effect is highly sensitive to changes in the molecular packing and, consequently, can be observed very rarely. This is consistent with the results of the previous study.[19] Hundreds of various derivatives of nitronyl nitroxides and metal complexes with these radicals have been already synthesized.[21] However, chemomechanical movements, *e.g.*, "jumps" at the macrolevel, are observed only for the crystals of $[M(hfac)_2L^{Im}{}_2]$ and related $[Cu(hfac)_2L^{CD_3}{}_2]$.

In conclusion, let us note that single crystals of the complexes $[Cu(hfac)_2L^{Im}{}_2]$, $[Co(hfac)_2L^{Im}{}_2]$, and $[Mn(hfac)_2L^{Im}{}_2]$ were grown and their structures have been solved earlier.[19] The corresponding experiment for $[Ni(hfac)_2L^{Im}{}_2]$ was not performed, because numerous attempts to grow high-quality single crystals of this compound failed. The resulting crystals were twins and gave virtually no reflections. Only in one recent experiment (see the Experimental section), we obtained intergrowths of single crystals, from one of which a single-crystal fragment was cut, which allowed us to obtain satisfactory X-ray diffraction data (see Tables 1 and 4). The crystal structure appeared to be similar to that of $[Cu(hfac)_2L^{Im}{}_2]$. Without considering in detail the data for the complex $[Ni(hfac)_2L^{Im}{}_2]$, we report only the distances between four O atoms of the nitronyl nitroxide moiety, which are similar to those presented in Fig. 2, *a* and *b*. For the complex $[Ni(hfac)_2L^{Im}{}_2]$, these distances are 4.186, 3.778, and 4.186 Å. A comparison of these values with the corresponding distances presented in Fig. 2, *a* and *b* shows that the distances between the oxygen atoms in the crystals of $[Ni(hfac)_2L^{Im}{}_2]$ are even more similar to those in $[Cu(hfac)_2L^{Im}{}_2]$ than the corresponding parameters for $[Cu(hfac)_2L^{CD_3}{}_2]$. Hence, it is not surprising that the crystals of $[Ni(hfac)_2L^{Im}{}_2]$ exhibit mechanical activity similar to that of the crystals of $[Cu(hfac)_2L^{Im}{}_2]$ (or $[Cu(hfac)_2L^{CD_3}{}_2]$). Therefore, the results of the X-ray diffraction study of the complex $[Ni(hfac)_2L^{Im}{}_2]$ confirm once again that the packing in heterospin crystals plays a key role in the appearance of chemomechanical activity. The features of the packing responsible for the appearance of chemomechanical movement of the crystals of $[M(hfac)_2L^{Im}{}_2]$ require special investigation, which we plan to perform in the near future.

Experimental

4,4,5,5-Tetramethyl-2-(1-methyl-1*H*-imidazol-5-yl)-4,5-dihydro-1*H*-imidazole-3-oxide-1-oxyl,[22] 2,3-dihydroxyamino-2,3-dimethylbutane,[23] 5-formyl-1-methyl-1*H*-1,2,3-triazole,[24,25] Cu^{II} and Ni^{II} hexafluoroacetylacetonates,[26,27] $[Cu_2(piv)_4(THF)_2]$,[28] and $[Co_2(piv)_4(H_2O)(Hpiv)_4]$ (see Ref. 29) were synthesized according to known procedures; commercial reagents and solvents were used as received. Acetone for the synthesis of L^{CD_3} was dried over Na_2SO_4. Microanalyses were carried out on an EURO EA3000 CHNS analyzer in the N. N. Vorozhtsov Novosibirsk Institute of Organic Chemistry of the Siberian Branch of the Russian Academy of Sciences. The magnetochemical measurements were performed on a Quantum

Design MPMSXL SQUID magnetometer in the temperature range of 2—300 K. The effective magnetic moment was calculated from the equation

$$\mu_{\mathrm{eff}}(T) = (8\chi'_{\mathrm{M}}T)^{1/2},$$

where χ'_{M} is the molar paramagnetic component of the magnetic susceptibility estimated from Pascal constants.[30]

2-(*N*-Trideuteriomethyl-1*H*-imidazol-5-yl)-4,4,5,5-tetramethyl-4,5-dihydro-1*H*-imidazole-3-oxide-1-oxyl ($\mathbf{L^{CD_3}}$). A solution of imidazole-4(5)-carbaldehyde (**1**) (0.76 g, 7.9 mmol) and $(CD_3)SO_4$ (1.0 g, 7.9 mmol) in acetone (50 mL) was stirred under reflux for 1 h. Then the reaction mixture was cooled, D_2O (1 mL) was added, and the mixture was neutralized with $NaHCO_3$. The product was extracted with $CHCl_3$ (10×5 mL). The combined extracts were dried with Na_2SO_4, filtered through a layer of Al_2O_3 (2×10 cm), and concentrated. A mixture of the resulting 5-formyl-*N*-trideuteriomethylimidazole (**2**) (0.29 g, 2.57 mmol) and 2,3-dihydroxyamino-2,3-dimethylbutane (**3**) (0.38 g, 2.57 mmol) in MeOH (2 mL) was stirred at room temperature for 2 h. Then the reaction mixture was kept at 5 °C for 10 h and concentrated. The residue was oxidized with MnO_2 (1.5 g) in MeOH (10 mL) for 2 h. The reaction mixture was filtered, the filtrate was concentrated, and the residue was crystallized from a hexane—ethyl acetate mixture. The yield was 0.26 g (14%), deep-blue crystals, m.p. 163—165 °C, R_f 0.33 (MeOH—AcOEt, 1 : 10). IR, ν/cm^{-1}: 542, 597, 626, 646, 668, 756, 826, 841, 865, 934, 1040, 1071, 1124, 1144, 1170, 1222, 1235, 1262, 1288, 1336, 1347, 1367, 1398, 1467, 1485, 1589, 2096, 2152, 2937, 2992, 3099. μ_{eff} = 1.73 μ_B (200—300 K). Found (%): C, 54.9; N, 23.3. $C_{11}H_{14}D_3N_4O_2$. Calculated (%): C, 55.0; N, 23.3. High-resolution MS, found: *m/z* 240.1536 $[M]^+$. $C_{11}H_{14}D_3N_4O_2$. Calculated: M = 240.1534. MS, *m/z* (I_{rel} (%)): 242 $[M + 2]^+$ (1.3), 241 $[M + 1]^+$ (13.4), 240 $[M]^+$ (100), 152 (5), 127 (7), 112 (30), 114 (8), 111 (21), 110 (10), 84 $[Me_2C—CMe_2]^+$ (57), 69 (50). High-resolution MS for L^{Im}, found: *m/z* 237.1345 $[M]^+$. $C_{11}H_{17}N_4O_2$. Calculated: M = 237.1346. MS, *m/z* (I_{rel} (%)): 239 $[M + 2]^+$ (1.3), 238 $[M + 1]^+$ (14.0), 237 $[M]^+$ (87), 149 (25), 124 (6), 114 (20), 109 (25), 108 (46), 107 (14), 84 $[Me_2C—CMe_2]^+$ (100), 69 (73).

2-(1-Methyl-1,2,3-triazol-5-yl)-4,4,5,5-tetramethyl-4,5-dihydro-1*H*-imidazole-3-oxide-1-oxyl ($\mathbf{L^{Tr}}$). A solution of 5-formyl-*N*-methyl-1*H*-1,2,3-triazole (**4**) (0.97 g, 8.73 mmol) and dihydroxyamine **3** (1.29 g, 8.73 mmol) in methanol (10 mL) was stirred for 7 h and concentrated. The crystalline product, which was obtained by triturating the residue with toluene (5 mL), was filtered off, and crude 1,3-dihydroxyimidazolidine **5** was obtained in a yield of 0.53 g. Then $NaIO_4$ (0.42 g, 2.0 mmol) was added portionwise to a stirred mixture of compound **5** (0.32 g, 1.3 mmol), CH_2Cl_2 (10 mL), and H_2O (4 mL) during 5 min. The reaction mixture was stirred for 20 min, the organic layer was removed, and the aqueous phase was extracted with CH_2Cl_2 (2×5 mL). The combined extracts were dried with Na_2SO_4 and concentrated. The residue was chromatographed on a column with SiO_2 (1.5×15 cm) using ethyl acetate as the eluent. The blue fraction was collected and concentrated. The residue was crystallized from a CH_2Cl_2—heptane mixture. The yield was 0.16 g (52%), m.p. 206—207 °C, R_f 0.56 (AcOEt). IR, ν/cm^{-1}: 409, 469, 481, 541, 618, 677, 701, 760, 821, 866, 882, 963, 1050, 1117, 1151, 1172, 1223, 1259, 1293, 1368, 1403, 1419, 1462, 1601, 2987, 3111, 3423. μ_{eff} = 1.73 μ_B (200—300 K). Found (%): C, 50.1; H, 6.6; N, 29.4. $C_{10}H_{16}N_5O_2$. Calculated (%): C, 50.4; H, 6.8; N, 29.4.

Bis(1,1,5,5-tetrafluoropentane-2,4-dionato)copper(II) ([Cu(tfac)$_2$]). A solution of $Cu(OAc)_2 \cdot H_2O$ (2.9 g, 0.015 mol) in water (50 mL) was added to a vigorously stirred mixture of Htfac (5.0 g, 0.029 mol) and water (100 mL), and then a solution of NaOH (1.1 g, 0.028 mol) in water (30 mL) was added during 30 min. The pale-green crystalline precipitate was filtered off, washed with water, and dried in air. The product was dissolved in EtOH (50 mL), and the resulting solution was diluted with water (150 mL). The crystals of $[Cu(tfac)_2(H_2O)]$ that formed were filtered off, washed with water, and dried in air. The dehydration of $[Cu(tfac)_2(H_2O)]$ was performed in a desiccator over $CaCl_2$. The yield was 4.2 g (71%). μ_{eff} = 1.87 μ_B (20—300 K). Found, %: C, 30.4; H, 1.2; F, 38.4. $C_{10}H_6CuF_8O_4$. Calculated (%): C, 29.6; H, 1.5; F, 37.5.

Bis(1,1,1,5,5,6,6,6-octafluorohexane-2,4-dionato)copper(II) ([Cu(pfh)$_2$]) was synthesized as described for the complex $[Cu(tfac)_2]$. The yield was 80%. Found (%): C, 25.2; H, 0.8; F, 51.3. $C_{12}H_2CuF_{16}O_4$. Calculated (%): C, 25.0; H, 0.4; F, 52.6. Crystals suitable for X-ray diffraction were obtained after the drying of $[Cu(pfh)_2(H_2O)]$ in a desiccator.

Bis(1,1,1,2,2,3,3,4,4,8,8,9,9,10,10,11,11,11-octadecafluoroundecane-5,7-dionato)copper(II) ([Cu(pfu)$_2$]) was synthesized as described for the complex $[Cu(tfac)_2]$. The yield was 86%. Found (%): C, 24.1; H, 0.1; F, 62.9. $C_{22}H_2CuF_{36}O_4$. Calculated (%): C, 24.5; H, 0.2; F, 63.5.

Bis(1,1,1,5,5,5-hexafluoropentane-2,4-dionato)bis[2-(*N*-trideuteriomethyl-1*H*-imidazol-5-yl)-4,4,5,5-tetramethyl-4,5-dihydro-1*H*-imidazole-3-oxide-1-oxyl]copper(II) ([Cu(hfac)$_2$L^{CD_3}$_2$]). A mixture of $Cu(hfac)_2$ (0.0199 g, 0.04 mmol) and L^{CD_3} (0.02 g, 0.08 mmol) was dissolved in CH_2Cl_2 (2 mL). Ethanol (3 mL) was carefully layered onto the reaction solution. The dark-blue needle-like crystals that formed after several hours were filtered off, washed with cold EtOH, and dried in air. The yield was 93%. The complex is readily soluble in Me_2CO, CH_2Cl_2, and $CHCl_3$ and poorly soluble in MeOH and EtOH. Found (%): C, 40.1; F, 23.4; N, 11.7. $C_{32}H_{30}CuD_6F_{12}N_8O_8$. Calculated (%): C, 40.1; F, 23.8; N, 11.7.

Bis(1,1,5,5-tetrafluoropentane-2,4-dionato)bis[4,4,5,5-tetramethyl-2-(1-methyl-1*H*-imidazol-5-yl)-4,5-dihydro-1*H*-imidazole-3-oxide-1-oxyl]copper(II) dichloromethane solvate ([Cu(tfac)$_2$L^{Im}$_2$] · 2CH$_2$Cl$_2$) was synthesized as described for the complex $[Cu(hfac)_2L^{CD_3}{}_2]$ in 90% yield. The complex loses solvent molecules in air. Found (%): C, 40.3; H, 4.3; F, 16.4; N, 11.1. $C_{34}H_{44}Cl_4CuF_8N_8O_8$. Calculated (%): C, 38.9; H, 4.2; F, 14.5; N, 10.7.

Bis(1,1,1,5,5,6,6,6-octafluorohexane-2,4-dionato)bis[4,4,5,5-tetramethyl-2-(1-methyl-1*H*-imidazol-5-yl)-4,5-dihydro-1*H*-imidazole-1-oxyl]copper(II) dichloromethane solvate ([Cu(pfh)$_2$L^{Im}$_2$] · 1/2CH$_2$Cl$_2$) was synthesized as described for the complex $[Cu(hfac)_2L^{CD_3}{}_2]$ in 99% yield. The complex loses solvent molecules in air. Found (%): C, 38.4; H, 3.7; F, 27.7; N, 10.2. $C_{34.5}H_{37}ClCuF_{16}N_8O_8$. Calculated (%): C, 37.9; H, 3.4; F, 27.8; N, 10.2.

Bis(1,1,5,5-tetrafluoropentane-2,4-dionato)bis[4,4,5,5-tetramethyl-2-(1-methyl-1*H*-imidazol-5-yl)-4,5-dihydro-1*H*-imidazole-3-oxide-1-oxyl]copper(II) ethanol solvate ([Cu(tfac)$_2$L^{Im}$_2$] · · 2EtOH). A solution of $Cu(tfac)_2$ (0.0214 g, 0.05 mmol) in EtOH (2 mL) was added to a solution of L^{Im} (0.025 g, 0.11 mmol) in EtOH (5 mL). The reaction mixture was kept at +5 °C. The blue-violet platelet crystals that formed after 15 h were filtered off, washed with cold EtOH, and dried in air. The yield was 0.0288 g (56%). The complex loses solvent molecules in air. Found (%): C, 43.5; H, 4.3; F, 17.6; N, 12.7. $C_{32}H_{40}CuF_8N_8O_8$. Calculated (%): C, 43.6; H, 4.6; F, 17.3; N, 12.8.

Tetrakis[(1,1,1,2,2,3,3,4,4,8,8,9,9,10,10,11,11,11-octadecafluoroundecane-5,7-dionato)]tris[4,4,5,5-tetramethyl-2-(1-methyl-1*H*-imidazol-5-yl)-4,5-dihydro-1*H*-imidazole-3-oxide-1-oxyl]dicopper(II) dichloromethane solvate ($[(Cu(pfu)_2)_2L^{Im}{}_3]\cdot1/2CH_2Cl_2$). A mixture of $[Cu(pfu)_2]$ (0.0341 g, 0.03 mmol) and L^{Im} (0.015 g, 0.06 mmol) was dissolved in CH_2Cl_2 (2 mL). The solution was concentrated by blowing its surface with air. The residue was dissolved in EtOH (5 mL), and the solution was kept at −18 °C. The dark-blue needle-like crystals that formed after several hours were filtered off, washed with cold EtOH, and dried in air. The yield was 52%. The complex is readily soluble in Me_2CO and CH_2Cl_2. Found (%): C, 32.8; H, 1.7; F, 46.8; N, 5.7. $C_{77}H_{55}Cu_2F_{72}N_{12}O_{14}$. Calculated (%): C, 32.3; H, 1.9; F, 47.7; N, 5.9 (for the desolvated sample).

Di[bis(1,1,1,5,5,5-hexafluoropentane-2,4-dionato)(2-(1-methyl-1,2,3-triazol-5-yl)-4,4,5,5-tetramethyl-4,5-dihydro-1*H*-imidazole-3-oxide-1-oxyl)copper(II)] dichloromethane solvate ($[Cu(hfac)_2L^{Tr}]_2\cdot CH_2Cl_2$). A mixture of $Cu(hfac)_2$ (0.02 g, 0.04 mmol) and L^{Tr} (0.01 g, 0.04 mmol) was dissolved in CH_2Cl_2 (3 mL), and then heptane (3 mL) was added. The solution was kept at +5 °C for several hours. The resulting dichroic (green-brown) crystals were filtered off, washed with cold heptane, and dried in air. The yield was 91%. Found (%): C, 34.2; H, 2.3; F, 31.5; N, 9.9. $C_{40}H_{36}Cu_2F_{24}N_{10}O_{12}$. Calculated (%): C, 33.6; H, 2.5; F, 31.8; N, 9.8 (for the desolvated sample). A small amount of crystals of $[Cu(hfac)_2L^{Tr}{}_2]$ were isolated from the mother liquor, and these crystals were studied by X-ray diffraction.

Bis(1,1,1,5,5,5-hexafluoropentane-2,4-dionato)bis[2-(1-methyl-1,2,3-triazol-5-yl)-4,4,5,5-tetramethyl-4,5-dihydro-1*H*-imidazole-3-oxide-1-oxyl]copper(II) ($[Cu(hfac)_2L^{Tr}{}_2]$). A mixture of $Cu(hfac)_2$ (0.02 g, 0.04 mmol) and L^{Tr} (0.02 g, 0.08 mmol) was dissolved in CH_2Cl_2 (3 mL). Then heptane (3 mL) was added, and the solution was kept at +5 °C. The large dark-green crystals that formed after several hours were filtered off, washed with cold heptane, and dried in air. The yield was 97%. Found (%): C, 37.8; H, 3.4; F, 24.0; N, 14.7. $C_{30}H_{34}CuF_{12}N_{10}O_8$. Calculated (%): C, 37.8; H, 3.6; F, 23.9; N, 14.7.

Bis[μ-(2,2-dimethylpropionato-*O*)]bis[4,4,5,5-tetramethyl-2-(1-methyl-1*H*-imidazol-5-yl)-4,5-dihydro-1*H*-imidazole-3-oxide-1-oxyl]copper(II) methanol solvate ($[Cu(piv)_2L^{Im}{}_2]\cdot2MeOH$). A solution of L^{Im} (0.07 g, 0.29 mmol) in MeOH (3 mL) was added to a solution of $[Cu_2(piv)_4(THF)_2]$ (0.05 g, 0.07 mmol) in MeOH (4 mL). The dichroic (dark green and green-violet) crystals that formed after 4 days were filtered off and washed with cold MeOH (2 mL). The yield was 0.1 g (90%). Found (%): C, 51.7; H, 7.0; N, 15.1. $C_{32}H_{52}CuN_8O_8$. Calculated (%): C, 51.9; H, 7.1; N, 15.1.

Bis[μ-(2,2-dimethylpropionato-*O*)]bis[4,4,5,5-tetramethyl-2-(1-methyl-1*H*-imidazol-5-yl)-4,5-dihydro-1*H*-imidazole-3-oxide-1-oxyl]cobalt(II) ($[Co(piv)_2L^{Im}{}_2]$). A solution of L^{Im} (0.055 g, 0.23 mmol) in CH_2Cl_2 (2 mL) was added to a solution of $[Co_2(piv)_4(H_2O)(Hpiv)_4]$ (0.11 g, 0.116 mmol) in CH_2Cl_2 (4 mL). The reaction mixture was filtered, and then hexane (3 mL) was slowly added. The dark-blue crystals that precipitated after 2 days were filtered off and washed with hexane (1 mL). The yield was 0.063 g (40%). Found (%): C 51.9; H, 7.3; N, 15.2. $C_{32}H_{52}CoN_8O_8$. Calculated (%): C, 52.2; H, 7.1; N, 15.2.

Bis(1,1,1,5,5,5-hexafluoropentane-2,4-dionato)bis[4,4,5,5-tetramethyl-2-(1-methyl-1*H*-imidazol-5-yl)-4,5-dihydro-1*H*-imidazole-3-oxide-1-oxyl]nickel(II) ($[Ni(hfac)_2L^{Im}{}_2]$). A solution of L^{Im} (0.019 g, 0.082 mmol) in toluene (3 mL) was added to a solution of $[Ni(hfac)_2(H_2O)_2]$ (0.021 g, 0.041 mmol) in a mixture of CH_2Cl_2 (3 mL) and toluene (1 mL). After 24 h, intergrowths of blue-green crystals that precipitated were filtered off, washed with toluene, and dried in flowing air. The yield was 0.015 g (38%). Found (%): C, 40.7; H, 4.1; F, 24.4; N, 11.8. $C_{32}H_{36}F_{12}N_8NiO_8$. Calculated (%): C, 40.6; H, 3.8; F, 24.1; N, 11.8.

X-ray diffraction study. The single-crystal X-ray diffraction data sets were collected on SMART APEX II and SMART APEX DUO (Bruker AXS) diffractometers (Mo-Kα radiation, λ = 0.71073 Å). Absorption corrections were applied with the use of the Bruker SADABS software, version 2.10. The structures were solved by direct methods and refined by the full-matrix least-squares method with anisotropic displacement parameters for all nonhydrogen atoms. The H atoms were positioned geometrically and refined using a riding model. All calculations were carried out with the use of the Bruker Shelxtl Version 6.14 software. The crystallographic characteristics and the X-ray data collection statistics are given in Tables 1—3. Selected bond lengths and bond angles are listed in Tables 4 and 5.

It should be noted that the disorder of the perfluoroalkyl groups in fluorinated β-diketonates sharply increases with increasing size and it is not reduced in low-temperature experiments. Due to this fact, we failed to obtain X-ray data for $[[Cu(pfu)_2]_2L^{Im}{}_3]\cdot1/2CH_2Cl_2$ with a satisfactory *R* factor and good geometry for the C_4F_9 group and, consequently, only crystallographic characteristics are given for this complex.

This study was financially supported by the Russian Foundation for Basic Research (Project Nos 11-03-12001 and 11-03-00027), the Council on Grants at the President of the Russian Federation (Program for State Support of Young Scientists, Grants MK-3112.2011.3 and MK-868.2011.3), the Russian Academy of Sciences, and the Siberian Branch of the Russian Academy of Sciences.

References

1. D. G. B. Boocock, R. Darcy, E. F. Ullman, *J. Am. Chem. Soc.*, 1968, **21**, 5945.
2. E. F. Ullman, J. H. Osiecki, D. G. B. Boocock, R. Darcy, *J. Am. Chem. Soc.*, 1972, **94**, 7049.
3. US Pat. 3927019; *Chem. Abstrs*, 1976, **84**, 180213.
4. V. I. Ovcharenko, in *Stable Radicals: Fundamentals and Applied Aspects of Odd-Electron Compounds*, Ed. R. Hicks, Wiley—VCH, New York, 2010, 461.
5. E. V. Tretyakov, V. I. Ovcharenko, *Usp. Khim.*, 2009, **78**, 1051 [*Russ. Chem. Rev. (Engl. Transl.)*, 2009, **78**, 971].
6. A. Caneschi, D. Gatteschi, R. Sessoli, P. Rey, *Acc. Chem. Res.*, 1989, **22**, 392].
7. V. I. Ovcharenko, R. Z. Sagdeev, *Usp. Khim.*, 1999, **68**, 381 [*Russ. Chem. Rev. (Engl. Transl.)*, 1999, **68**, 345].
8. O. Kahn, *Acc. Chem. Res.*, 2000, **33**, 647.

9. H. Iwamura, K. Inoue, T. Hayamizu, *Pure Appl. Chem.*, 1996, **68**, 243.
10. D. Luneau, P. Rey, *Coord. Chem. Rev.*, 2005, **249**, 2591.
11. K. E. Vostrikova, *Coord. Chem. Rev.*, 2008, **252**, 1409.
12. D. Luneau, A. Borta, Y. Chumakov, J.-F. Jacquot, E. Jeanneau, C. Lescop, P. Rey, *Inorg. Chim. Acta*, 2008, **361**, 3669.
13. D. Gatteschi, R. Sessoli, J. Villain, *Molecular Nanomagnets*, Oxford University Press, Oxford, 2006, 395.
14. H. Iwamura, K. Inoue, in *Magnetism: Molecules to Materials II. Molecule-Based Materials*, Eds J. S. Miller, M. Drillon, Wiley—VCH, Weinheim, 2001, 61.
15. H. Oshio, T. Ito, *Coord. Chem. Rev.*, 2000, **198**, 329.
16. L. Ouahab, *Coord. Chem. Rev.*, 1998, **178—180**, 1501.
17. E. Yu. Fursova, V. I. Ovcharenko, *Zh. Ross. Khim. Obshch. im. D. I. Mendeleeva*, 2009, **LIII**, 23 [*Mendeleev Chem. J.* (*Engl. Transl.*), 2009, **LIII**].
18. O. Sato, J. Tao, Y.-Z. Zhang, *Angew. Chem.*, *Int. Ed.*, 2007, **46**, 2152.
19. V. I. Ovcharenko, S. V. Fokin, E. Yu. Fursova, O. V. Kuznetsova, E. V. Tretyakov, G. V. Romanenko, A. S. Bogomyakov, *Inorg. Chem.*, 2011, **50**, 4307.
20. W. Sakami, D. W. Wilson, *J. Biol. Chem.*, 1944, **154**, 215.
21. *Cambridge Structural Database System*, Release 2010 (updated, May 2011).
22. V. Ovcharenko, E. Fursova, G. Romanenko, I. Eremenko, E. Tretyakov, V. Ikorskii, *Inorg. Chem.*, 2006, **45**, 5338.
23. V. I. Ovcharenko, S. V. Fokin, G. V. Romanenko, I. V. Korobkov, P. Ray, *Izv. Akad. Nauk, Ser. Khim.*, 1999, 1539 [*Russ. Chem. Bull. (Engl. Transl.)*, 1999, **48**, 1519].
24. US Pat. 6255305 B1; *Chem. Abstrs*, 1998, **184**, 167433.
25. Int. Appl. WO 135826 A2; *Chem. Abstrs*, 2008, **149**, 556635.
26. J. A. Bertrand, R. I. Kaplan, *Inorg. Chem.*, 1966, **5**, 489.
27. V. I. Ovcharenko, K. E. Vostrikova, A. V. Podoplelov, R. Z. Sagdeev, G. V. Romanenko, V. N. Ikorskii, *Polyhedron*, 1994, **13**, 2781.
28. T. O. Denisova, E. V. Amel´chenkova, I. V. Pruss, Zh. V. Dobrokhotova, O. P. Fialkovskii, S. E. Nefedov, *Zh. Neorg. Khim.,* 2006, **51**, 1098 [*Russ. J. Inorg. Chem.* (*Engl. Transl.*), 2006, **51**].
29. G. Aromi, A. C. Batsanov, P. Christian, M. Helliwell, A. Parkin, S. Parsons, A. A. Smith, G. A. Timco, R. E. P. Winpenny, *Chem. Eur. J.*, 2003, **9**, 5142.
30. L. Carlin, *Magnetochemistry*, Springer-Verlag, Berlin, 1986.

Received July 12, 2011;
in revised form November 10, 2011